PAPER

Check for updates

Enhancing the dimethyl ether carbonylation performance over hydrogen-type mordenites modified by pyrazole hydrochloride

Yiyin Liu, Yiyang Shen, Jianming Geng and Xinfa Dong [ID] *

Hydrogen-type mordenite (HMOR) modified with pyrazole hydrochloride (Pya·HCl) was prepared by the ion exchange method. The results showed that Pya·HCl introduction significantly improved the activity and stability of HMOR in the carbonylation reaction of dimethyl ether (DME) to methyl acetate (MA). Small pyrazole ions (HPya$^+$) entered into the twelve-membered ring (12-MR) pores of HMOR and selectively replaced part of the Brønsted acid (BAS), thus suppressing the formation of carbon deposits. The modified HMOR presented a larger specific surface area and pore volume, which provided larger channels for molecular diffusion. Additionally, non-framework aluminum was removed by the acidic Pya·HCl solution, resulting in the formation of mesopores, which facilitated the migration of carbon-deposited species from the inside of the zeolite to the outside.

1. Introduction

The zeolite-catalyzed carbonylation of dimethyl ether (DME) provides a non-noble metal-catalyzed and halogen-free method to produce high value-added methyl acetate (MA), ethanol and carbon resources from carbon resources such as coal, natural gas and renewable biomass.[1,2] Since this catalytic reaction was first reported by Iglesia and colleagues,[1] many zeolites, including hydrogen-type mordenite (HMOR), H-ZSM-35, H-ZSM-5, and H-EU-10, have been extensively investigated.[3] Among them, HMOR has the highest carbonylation activity because of its unique framework structure.[4,5] It is believed that the carbonylation of DME occurs mainly in the 8-MR channel of HMOR, and its special quantum confinement effect gives HMOR extremely high MA selectivity. The Brønsted acid (BAS) in the 12-MR channel is a carbon deposit reaction site and easily accumulates carbon, resulting in the rapid inactivation of HMOR during carbonylation.[5] Therefore, precise adjustment of the distribution of acid sites in HMOR or selective BAS shielding in the 12-MR channel is essential for improving the activity and stability of carbonylation.

Li *et al.*[6] synthesized a series of cerium-containing MORs samples by a one-step hydrothermal method. The aluminum in the zeolite framework is isomorphously replaced by Ce^{3+} species, resulting in BAS enrichment in 8-MR and thus improving carbonylation activity. Liu *et al.* employed large-volume cations such as trimethylamine ions (TMA$^+$)[7] and alky-limidazolium ions[8] to conduct ion exchange with HMOR and

selectively replace the carbon deposit active center in the 12-MR channel. The bulk of cations replace the BAS (H$^+$) in the 12-MR channel, while the BAS (H$^+$) in the 8-MR channel is not affected. TMA$^+$ acts as the equilibrium charge of the 12-MR channel and shields the active sites of carbon deposits. The modified HMOR exhibits good stability for the carbonylation reaction. However, the Brunauer–Emmett–Teller (BET) specific surface area of the modified sample was only less than 1/10 of the original due to the serious blockage of pores by TMA$^+$ cations, and the large-volume cations may acid-shield the BAS of the aluminum oxide tetrahedron at the junction of 12-MR and 8-MR, resulting in a significant decrease in activity. Li *et al.*[9] showed that the interaction of non-framework aluminum with adjacent BAS sites will form a strong Lewis acid (LAS). Moreover, non-framework aluminum species play an important role in hydrogen transfer and C–C bond formation,[10] which means that non-framework aluminum will work in concert with BAS to accelerate the formation of carbon deposits in the DME carbonylation reaction. Wang *et al.*[11] performed simple alkali treatment on MOR synthesized by the template method to remove a certain amount of silicon species and a small amount of aluminum species, resulting in the formation of mesopores and macropores and the improvement in the mass transfer efficiency. The single-pass lifespan of MOR was gradually extended. Reule *et al.*[12] used nitric acid to carry out selective four-membered ring dealumination of MOR, which also showed that the removal of non-framework aluminum is beneficial to the carbonylation of DME. Huang *et al.*[13] proposed to block the coking centers of mordenite with pyridine. The results indicated that the concentration of BAS strongly affects the stability of pyridine adsorption. The coke intermediate formed in the 12-

Guangdong Provincial Key Lab of Green Chemical Product Technology, School of Chemistry and Chemical Engineering, South China University of Technology, Guangzhou 510640, P. R. China. E-mail: cexfdong@scut.edu.cn

MR will lead to the desorption of adjacent adsorbed pyridine due to steric hindrance effect, thus accelerating deactivation.

Pyrazole is a smaller nitrogen-containing heterocyclic compound with a molecular diameter of 0.434 nm. It would be more difficult to pass through the 8-MR tunnel with a diameter of 0.26×0.57 nm and easier to enter the 12-MR tunnel with a diameter of 0.65×0.7 nm to shield the active sites of carbon deposits. Moreover, weakly basic pyrazole reacts with hydrochloric acid to form an aqueous solution of pyrazole hydrochloride (Pya·HCl), which can achieve the same function of removing non-framework aluminum in HMOR as nitric acid.[12] Here, pyrazole hydrochloride was used to modify HMOR for the carbonylation of DME by the ion exchange method. The results showed that the modified HMOR exhibited excellent carbonylation activity and stability.

2. Experimental

2.1 Preparation of catalyst

The parent HMOR with a silicon-to-aluminum ratio of 15 was purchased from Wuhan Zhizhen Molecular Sieve Company. The HMOR sample was calcined in air at 550 °C to remove organic impurities.

Pya·HCl-modified HMOR was prepared by the ion exchange method. 2 g HMOR sample was mixed with 20 mL Pya·HCl solution with different concentrations and placed in a water bath at 80 °C for ion exchange for 1 h. After filtration, the sample was washed with deionized water three times, and dried at 120 °C overnight. The final sample is denoted as HMOR-Pya-x, where x is the molar concentration of the Pya·HCl solution used for HMOR modification ($x = 0.35, 0.85, 1.3, 3.0$).

For comparison, HMOR treated only with 1.3 mol L^{-1} hydrochloric acid solution was prepared by the same procedure, and recorded as HMOR-HCl-1.3.

2.2 Characterization

Diffuse reflectance spectroscopy (DRS) was conducted using a Hitachi U-3010 36 dual-beam UV-Vis spectrometer equipped with an integrating sphere for sample composition analysis. A German NETZSCH thermogravimetric analyzer was employed to analyze the organic matter, such as pyrazole and carbon deposits, in the sample. The IR experiment was carried out on a Vertex 33-IR infrared spectrometer produced by Bruker, Germany. The Py-IR experiment was performed on a Bruker Tensor-27 FT-IR spectrometer with a resolution of 4 cm^{-1}. A nitrogen adsorption–desorption isotherm was obtained at -196 °C using a Micromeritics ASAP2020 instrument. The Brunauer–Emmett–Teller (BET) model was used to estimate the surface area of the sample. The pore volume of the sample was calculated by the Barrett–Joyner–Halenda (BJH) method. The powder XRD pattern was recorded on a D8 ADVANCE X-ray diffractometer with Cu-Kα radiation ($\lambda = 0.15418$ nm) at 40 kV and 40 mA.

2.3 DME carbonylation reaction

The modified HMOR catalyst sample was pressed and sieved to 40–60 mesh. 0.25 g catalyst was loaded into a fixed-bed stainless steel reactor with an inner diameter of 6 mm. Before the reaction, the catalyst was dried at 240 °C with nitrogen flow rate of 20 mL min^{-1} for 1 h. After the catalyst bed was cooled to the reaction temperature of 215 °C, the reactant mixture (4% DME, 76% CO, and 20% N$_2$) was introduced into the reactor with the gas hourly space velocity (GHSV) of 4800 mL (g^{-1} h^{-1}). The reaction pressure was then increased to 1.5 MPa. The effluents of the reactor were analyzed by an online Agilent 4890 gas chromatograph equipped with a capillary column (APPARATUS 0807242514). The conversion rate of DME (X_{DME}) and the selectivity (S_i) of each component were calculated according to the principle of carbon balance and the correction area normalization method.

$$X_{DME} = \frac{\sum_{k=2}^{5} A_k \times f_{M(k/DME)} + \sum A_{C_nH_m}}{\sum_{k=1}^{5} A_k \times f_{M(k/DME)} + \sum A_{C_nH_m}} \times 100\% \quad (1)$$

$$S_i = \frac{A_i \times f_{M(i/DME)}}{\sum_{k=2}^{5} A_k \times f_{M(k/DME)} + \sum A_{C_nH_m}} \times 100\% \quad (2)$$

where A_i is the chromatographic peak area of DME, methanol, ethanol, MA and ethyl acetate components ($i = 1, 2, 3, 4,$ and 5), $f_{M(i/DME)}$ is the molar correction factor of component i relative to that of DME, and C_nH_m is the hydrocarbon byproduct.

3. Results and discussion

3.1 Catalytic performance

Fig. 1(a) shows the change curve of the DME conversion rate with reaction time (TOS) in the carbonylation reaction of the samples. The highest DME conversion rates of the unmodified HMOR and the HMOR treated only with hydrochloric acid were 25% and 36%, respectively, and both showed rapid inactivation. With increasing Pya·HCl solution concentration, the carbonylation reaction activity of the HMOR catalyst modified by Pya·HCl gradually improved. However, when the concentration of Pya·HCl exceeded 1.3 mol L^{-1}, the catalyst activity increased very slowly, and the conversion of DME nearly reached its maximum value of 77%.

Fig. 1(b) illustrates the curve of the MA selectivity over time in the carbonylation reaction of catalyst samples. The MA selectivity of the carbonylation reaction of the modified HMOR gradually increased with increasing Pya·HCl solution concentration in the ion exchange process. When the concentration of Pya·HCl was greater than 0.85 mol L^{-1}, the selectivity of MA was greater than 95%.

3.2 Catalyst characterization

3.2.1 UV-Vis analysis. Fig. 2 presents the UV-Vis spectrophotometric curve of the unmodified HMOR and the HMOR-Pya-1.3 sample. The absorption peak at 206 nm was attributed to HMOR,[14] and the absorption peak of HMOR modified with Pya·HCl appeared at 214 nm. The absorption peak of pyrazole in the near ultraviolet region of 200–400 nm was corresponded
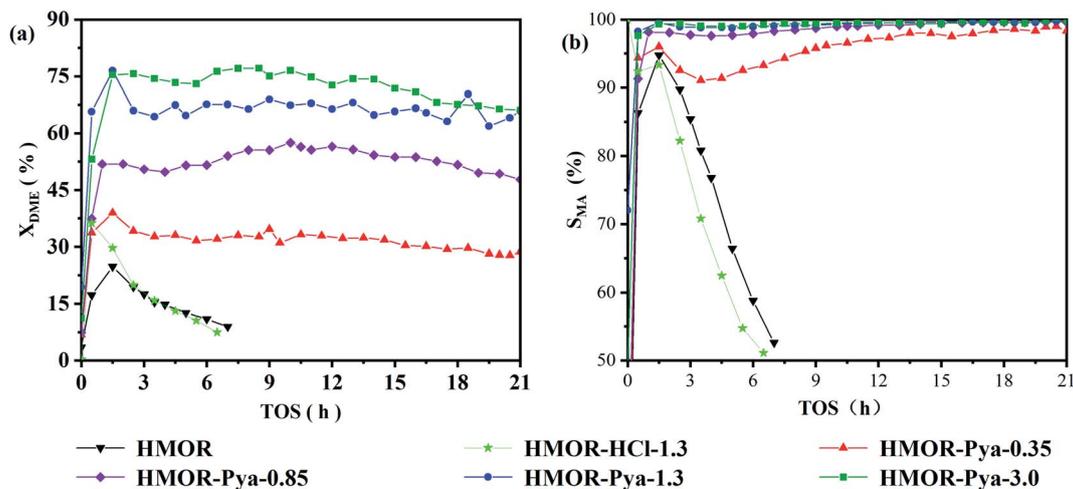
Fig. 1 (a) DME conversion rate and (b) MA selectivity of HMOR-Pya-x samples vs. reaction time.

to the $\pi \rightarrow \pi^*$ transition at 211 nm. In a strongly acidic environment, pyrazole molecules bound to –OH in the form of HPya$^+$, which redshifted the frequency of the maximum absorption wavelength by 3 to 4 nm.[15] This means that the absorption peak located at 214 nm was caused by the $\pi \rightarrow \pi^*$ transition of HPya$^+$ formed by the combination of pyrazole and BAS in the 12-MR channel of HMOR. In other words, the UV-Vis spectra demonstrated that HPya$^+$ was successfully introduced into the 12-MR channel of HMOR, replacing part of H$^+$ (shielding part of the BAS). It can be concluded that part of the BAS in the 12-MR channel of modified HMOR was shielded by HPya$^+$, which reduced the active centers of the carbon deposits reaction and improved the stability of the DME carbonylation reaction.

3.2.2 IR and Py-IR analysis. Fig. 3(a) exhibits the infrared absorption spectrum of the HMOR-Pya-x samples (x = 0, 0.35, 1.3, 3.0) in the wavenumber range of 2000–4000 cm^{-1}. The absorption peak at 3660 cm^{-1} was corresponded to the O–H

stretching vibration of the extraframework Al atoms.[11] The figure clearly shown that the intensity of the characteristic peak at 3660 cm^{-1} weakened as the concentration of the Pya·HCl solution increased, but when the concentration of the Pya·HCl solution was greater than 1.3 mol L^{-1}, the stretching vibration peak at 3660 cm^{-1} did not continue to weaken. This was consistent with the activity test results of the Pya·HCl-modified HMOR catalyst. As the concentration of the Pya·HCl solution increased, the –OH carbon deposit side reaction active centers of the extraframework Al atoms of HMOR were removed more thoroughly, and the catalyst exhibited better activity and selectivity. When the concentration of the Pya·HCl solution increased to a certain extent, the terminal –OH group of the extraframework Al atoms of HMOR was basically completely removed, so the absorption peak at 3660 cm^{-1} no longer decreased, and the catalyst activity and stability also tended to reach their optimal values.

In the Py-IR test of mordenite, only acid sites on the outer surface of mordenite and 12-MR pores can be detected because due to pyridine has a molecular kinetics diameter of 0.6 nm.[16] Fig. 3(b) displays the Py-IR spectrum and BAS content of the Pya-M-x samples (x = 0, 0.35, 3.0). Surprisingly, the characteristic peaks of both the BAS at approximately 1540 cm^{-1} and LAS at approximately 1450 cm^{-1} increased sharply after HMOR was treated with only a lower concentration of Pya·HCl solution (x = 0.35), which meant that the BAS and LAS amounts greatly increased. However, both the BAS and LAS characteristic peaks showed a gradual decrease as the concentration of Pya·HCl continued to increase, indicating that the amount of BAS and LAS gradually decreased. Reule's[12] work shown that there was certain non-framework aluminum fragments in the 12-MR orifice, which almost completely hindered the diffusion of molecules in the pores of the molecular sieve. Therefore, the pyridine molecules could not touch the internal acid sites during the pyridine infrared test, which exhibited relatively low acid content characteristics. When the HMOR catalyst was modified by Pya·HCl solution, the acidic low-concentration
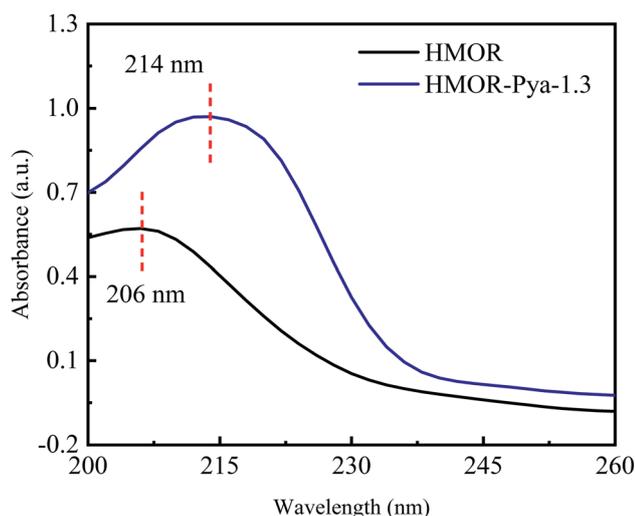

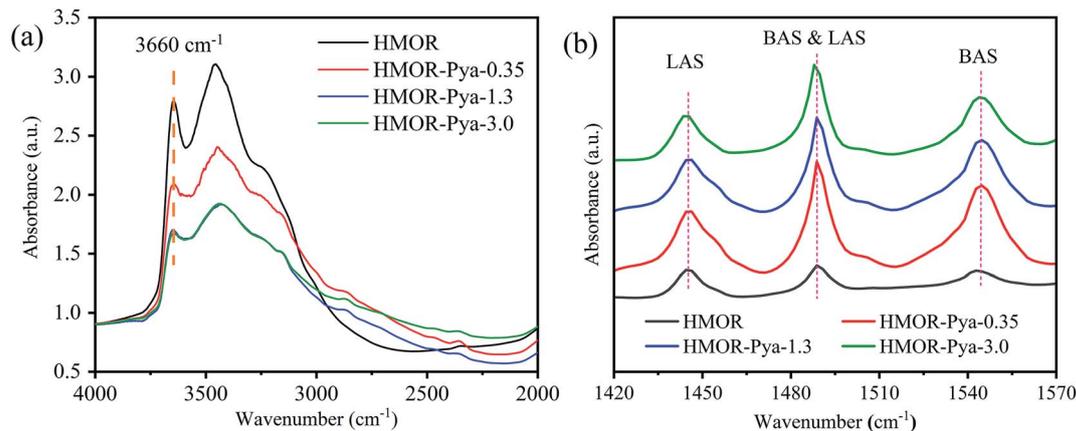**Fig. 2** UV-Vis spectra of HMOR & HMOR-Pya-1.3.

Fig. 3 (a) IR spectrum and (b) Py-IR spectrum of HMOR-Pya-x samples (x = 0, 0.35, 1.3, 3.0).

Pya·HCl solution could also remove the non-framework aluminum in the pores of 12-MR. In the meanwhile, the low-concentration pyrazole and HMOR were not completely exchanged, more pyridine molecules could enter 12-MR and combine with the BAS or LAS in the MR channel, resulting in a relatively high acid content. As the concentration of Pya·HCl solution increased, H^+ in the 12-MR channel was further replaced by $HPya^+$, the acid content presented a decreasing trend. The Py-IR characterization results indicated that the non-framework aluminum in the pores of 12-MR was removed after HMOR was treated with Pya·HCl solution. $HPya^+$ successfully entered the pores of 12-MR to replace the BAS, the active center of carbon deposition side reaction. Compared with previous results,[12] the replacement of nitric acid for removing non-framework aluminum in HMOR with larger heterocyclic compound (Pya·HCl) provided certain selectivity in affecting mostly carbon deposit active centers in 12-MR tunnel without much effect on 8-MR tunne due to the steric hindrance effect of bigger reagent. As a result, the catalyst lifetime was prolonged and selectivity of the MA formation was also increased upon partial removal of the nonframework aluminum in HMOR.

3.2.3 BET test. As shown in Fig. 4, the HMOR-Pya-x samples (x = 0, 0.35, 1.3, 3.0) exhibits a type I adsorption isotherm and an H4-type hysteresis loop, indicating that the samples had a typical microporous structure and an irregular mesoporous structure. The inset of Fig. 4 shows the pore size distribution of the HMOR-Pya-x samples. The number of mesopores in unmodified samples was very small in the range of 2–7 nm. In contrast, the number of mesopores in this range increased after modification, but decreased slightly with the increase of pyrazole hydrochloride concentration, because more $HPya^+$ became the equilibrium charge of the aluminum oxide tetrahedron. These results indicated that the non-framework aluminum in HMOR is removed, and more mesoporous structures are formed after HMOR is treated with acidic pyrazole hydrochloride solution, which was consistent with Reule's results.[12] The existence of mesopores made carbon deposits to diffuse out of the pores of the zeolite in time, and prevented the

carbon deposits from further condensing and blocking the pores. Therefore, although the HMOR-Pya-x samples still produce carbon deposits, they exhibited a relatively stable carbonylation performance.

The texture properties of HMOR-Pya-x samples (x = 0, 0.35, 1.3, 3.0) are summarized in Table 1. It can be clearly seen that both the specific surface area and pore volume showed a decreasing trend as the concentration of the Pya·HCl solution increased, which was because more H^+ in the HMOR channels was replaced by larger $HPya^+$ when the concentration of Pya·HCl solution increased. This was coincided with experiments of Liu et al.[8] However, as ion exchange gradually reached an equilibrium state, the specific surface area and pore volume
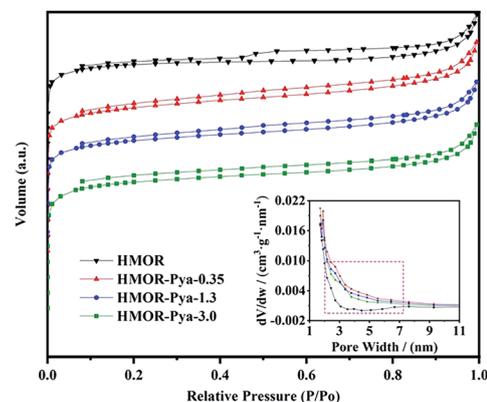

Fig. 4 N$_2$ adsorption–desorption isotherm and pore size distribution of HMOR-Pya-x samples (x = 0, 0.35, 1.3, 3.0).

Table 1 Texture properties of HMOR-Pya-x samples

Samples	$S_{BET}/(m^2\ g^{-1})$	$V_{micro}/(cm^3\ g^{-1})$
HMOR	429.5	0.167
HMOR-Pya-0.35	354.1	0.133
HMOR-Pya-1.3	335.9	0.127
HMOR-Pya-3.0	313.3	0.122

decreased at a lower rate. Obviously, the modified HMOR still had a large specific surface area and pore volume.

3.2.4 XRD analysis. Fig. 5 shows the XRD spectrum of the HMOR-Pya-x samples (x = 0, 0.35, 1.3, 3.0). Compared with the XRD standard card of unmodified HMOR, the 2θ and peak intensity of the characteristic diffraction peak of the HMOR-Pya-x samples exhibited no obvious change, indicating that the crystalline structure and crystallinity of HMOR were basically unchanged after ion exchange modification with Pya·HCl solution. In other words, in the ion exchange process, the purpose of removing non-framework aluminum and producing mesopores is achieved without destroying the basic structure of the molecular sieve.

3.2.5 TG analysis. Fig. 6(a) presents the TG and DTG curves of the fresh HMOR and HMOR-Pya-1.3 samples, respectively. The weight loss at temperatures below 250 °C is caused by the evaporation of adsorbed water.[7] No significant weight loss peak was observed for HMOR when the temperature is greater than 250 °C, which indicated that most of the internal organic template in HMOR was removed during calcination. However, the DTG curve of fresh HMOR-Pya-1.3 sample presented an obvious weight loss plateau at temperatures of 180–350 °C, which meant that pyrazole bound tightly to HMOR and was difficult to desorb. In addition, there are two weight loss peaks

in the DTG curve of fresh HMOR-Pya-1.3 sample. The weight loss peak at 523 °C was attributed to the combustion and carbonization of pyrazole,[7] while the weight loss peak corresponding to 681 °C might be caused by the combustion of carbon formed after the carbonization of pyrazole.

Fig. 6(b) depicts the TG and DTG curves of the spent HMOR and spent HMOR-Pya-1.3 samples after 21 hours of reaction. The TG curve shows that the weight loss rate of the spent HMOR-Pya-1.3 was significantly lower than that of the spent HMOR. In addition, the DTG curve of spent HMOR catalyst had two weight loss peaks when the temperature was greater than 180 °C. The small peak corresponding to 351 °C was attributed to the combustion of soft carbon deposits, and the larger peak at 628 °C is attributed to the combustion of hard carbon deposits.[7] Unmodified HMOR produced a large amount of hard coke, which severely restricted the molecular diffusion process and led to rapid deactivation. The DTG curve of spent HMOR-Pya-1.3 sample only shown three smaller weight loss peaks when the temperature was greater than 180 °C. The peak at 351 °C is attributed to the weight loss peak of soft carbon deposits and can be ignored. The combustion peak at 495 °C was attributed to the combustion of Pya,[7] and the peak at 655 °C was belonged to the combustion of hard carbon deposits.[7] The hard carbon content of the HMOR-Pya-1.3 decreased obviously. This was due to BAS shielding by HPya$^+$ in the 12-MR channel. As a result, the stability of the catalyst was significantly improved. In summary, the introduction of HPya$^+$ into the 12-MR channel of HMOR greatly reduced the amount of carbon deposits, which inhibited the formation of hard carbon deposits and improved the stability of carbonylation.
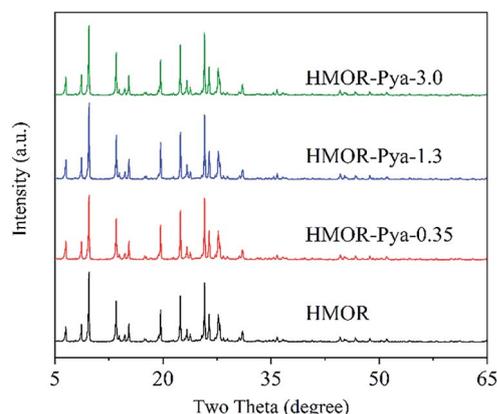
4. Conclusions

In summary, HMOR was successfully modified with larger heterocyclic compound (pyrazole hydrochloride, Pya·HCl) by the ion exchange method. The partial removal of the non-framework aluminum in HMOR by Pya·HCl provided certain selectivity in affecting mostly carbon deposit active centers in 12-MR tunnel without much effect on 8-MR tunnel. The HPya$^+$ selectively replaced part of the BAS centers in 12-MR, while retaining large diffusion channels to provide space for the

Fig. 5 XRD spectrum of HMOR-Pya-x samples (x = 0, 0.35, 1.3, 3.0).
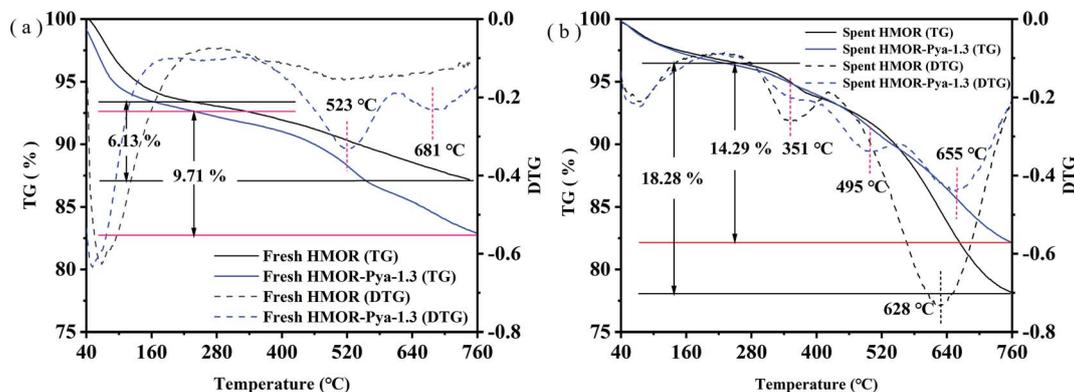

Fig. 6 TG and DTG curves of (a) fresh HMOR & HMOR-Pya-1.3 samples, and (b) spent HMOR & HMOR-Pya-1.3 catalysts.

diffusion of reactant molecules, thereby inhibiting carbon deposits without hindering the carbonylation reaction. Meanwhile, the non-framework aluminum in HMOR was effectively removed in the ion-exchange process to obtain more mesopores, which provided the channels for the diffusion of carbon deposits, reduced the accumulation of carbon deposits in the zeolite, and enhanced the stability of the carbonylation reaction.

Conflicts of interest

There are no conflicts to declare.

Acknowledgements

References

1 P. Cheung, A. Bhan, G. J. Sunley and E. Iglesia, *Angew. Chem., Int. Ed.*, 2006, **45**, 1617–1620.

2 P. Cheung, A. Bhan, G. J. Sunley, D. J. Law and E. Iglesia, *J. Catal.*, 2015, **245**, 110–123.

3 K. Fujimoto, T. Shikada, K. Omata and H. O. Tominaga, *Chem. Lett.*, 1984, **13**, 2047–2050.

4 J. E. Lewis, C. C. Freyhardt and M. E. Davis, *J. Phys. Chem. A*, 1996, **100**, 5039–5049.

5 A. Bhan and E. Iglesia, *Acc. Chem. Res.*, 2008, **41**, 559–567.

6 Y. Li, S. Huang, Z. Cheng, S. Wang, Q. Ge and X. Ma, *J. Catal.*, 2018, **365**, 440–449.

7 S. Liu, H. Liu, X. Ma, Y. Liu, W. Zhu and Z. Liu, *Catal. Sci. Technol.*, 2020, **10**, 4663–4672.

8 S. Liu, X. Fang, Y. Liu, H. Liu, X. Ma, W. Zhu and Z. Liu, *Catal. Commun.*, 2020, **147**, 106161.

9 S. Li, S. J. Huang, W. Shen, H. Zhang, H. Fang, A. Zheng, S. B. Liu and F. Deng, *J. Phys. Chem. C*, 2008, **112**, 14486–14494.

10 S. Müller, Y. Liu, F. M. Kirchberger, M. Tonigold, M. Sanchez-Sanchez and J. A. Lercher, *J. Am. Chem. Soc.*, 2016, **138**, 15994–16003.

11 X. Wang, R. Li, C. Yu, Y. Liu, L. Zhang, C. Xu and H. Zhou, *Fuel*, 2019, **239**, 794–803.

12 A. A. Reule, J. A. Sawada and N. Semagina, *J. Catal.*, 2017, **349**, 98–109.

13 Y. Li, Q. Sun, S. Huang, Z. Cheng, K. Cai, J. Lv and X. Ma, *Catal. Today*, 2018, **311**, 81–88.

14 N. Zhao, Y. Tian, L. Zhang, Q. Cheng, S. Lyu, T. Ding, Z. Hu, X. Ma and X. Li, *Chin. J. Catal.*, 2019, **40**, 895–904.

15 Y. Shi, Z. Wu, L. Chen, G. Chen, Y. Liu and L. Zhang, *Spectrosc. Spectral Anal.*, 2009, **29**, 781–785, DOI: 10.3964/j.issn.1000-0593(2009)03-0781-05.

16 Z. Hasan, M. Tong, B. K. Jung, I. Ahmed, C. Zhong and S. H. Jhung, *J. Phys. Chem. C*, 2014, **118**, 21049–21056.

© 2022 The Author(s). Published by the Royal Society of Chemistry